Updated Determination of Stress Parameters for Nine Well-Recorded Earthquakes in Eastern North America

David M. Boore
U.S. Geological Survey

ABSTRACT

Stress parameters ($\Delta\sigma$) are determined for nine relatively well-recorded earthquakes in eastern North America for ten attenuation models. This is an update of a previous study by Boore *et al.* (2010). New to this paper are observations from the 2010 Val des Bois earthquake, additional observations for the 1988 Saguenay and 2005 Riviere du Loup earthquakes, and consideration of six attenuation models in addition to the four used in the previous study. As in that study, it is clear that $\Delta\sigma$ depends strongly on the rate of geometrical spreading (as well as other model parameters). The observations necessary to determine conclusively which attenuation model best fits the data are still lacking. At this time, a simple $1/R$ model seems to give as good an overall fit to the data as more complex models.

INTRODUCTION

Within the context of stochastic-method ground-motion simulations, the stress parameter ($\Delta\sigma$) is of fundamental importance in simulations of ground motions at frequencies of engineering interest, as it and the seismic moment of the earthquake largely determine the amplitude of high-frequency radiation from earthquake sources (*e.g.*, Boore 2003). In an earlier study, Boore *et al.* (2010) (hereafter Bea10) determined $\Delta\sigma$ for eight relatively well-recorded earthquakes in eastern North America (ENA) by inverting 5%-damped pseudo-absolute response spectral acceleration (PSA) at periods of 0.1s and 0.2s. One of the key findings of that study is that $\Delta\sigma$ is closely tied to the attenuation model (as parameterized by geometrical spreading and Q). Since the publication of Bea10, the well-recorded **M** 5.1 Val des Bois, Canada, earthquake occurred on 23 June 2010, providing important data for determining $\Delta\sigma$ and thus increasing by about 20% the number of stress-parameter determinations in ENA for earthquakes greater than or equal to **M** 5. In addition, new data have been added to the datasets of several of the earthquakes previously studied, and several attenuation models have been newly proposed for use in ENA. For these reasons it is an opportune time to determine $\Delta\sigma$ for these attenuation models for the Val des Bois earthquake, as well as the earthquakes previously studied in Bea10.

EARTHQUAKES, STATIONS, AND PSA VALUES

Information concerning the earthquakes studied in this paper is given in Table 1. I focus on the Saguenay, Riviere du Loup, and Val des Bois earthquakes, although I redetermined $\Delta\sigma$ for the six other earthquakes considered in Bea10. The Saguenay earthquake is of interest because most previous interpretations have assigned a very high stress parameter to this event; the Riviere du Loup and Val des Bois earthquakes are recent **M** ≈ 5 earthquakes in ENA and were quite well recorded, at least at distances beyond about 30 km.

The data used in this paper are intended to include only those recordings at hard rock stations. To classify the stations from which data might be used, I relied primarily on the site classes given in the Engineering Seismology Toolbox (ESTB) (Assatourians and Atkinson 2010). For some of the sites, Boatwright and Seekins (2011) (BS11) and Boatwright (personal communication 2011) have reassigned hard rock ESTB sites to softer sites (and in a few cases, the other way around). I show $\Delta\sigma$ without and with the BS11 and Boatwright reclassifications.

TABLE 1
Event Information*

Date	Name	Depth (km)	M
1985-12-23	Nahanni	8	6.8
1988-11-25	Saguenay	29	5.8
1990-10-19	Mt. Laurier	13	4.7
1997-11-06	Cap Rouge	22	4.4
1999-03-16	St. Anne des Monts	19	4.5
2000-01-01	Kipawa	13	4.7
2002-04-20	Ausable Forks	11	5.0
2005-03-06	Riviere du Loup	13	4.7
2010-06-23	Val des Bois	22	5.1

* For all but Val des Bois, the information is from Boore *et al.* (2010); for Val des Bois, the source of the depth and moment magnitude are given in the Data and Resources section.

doi: 10.1785/gssrl.83.1.190

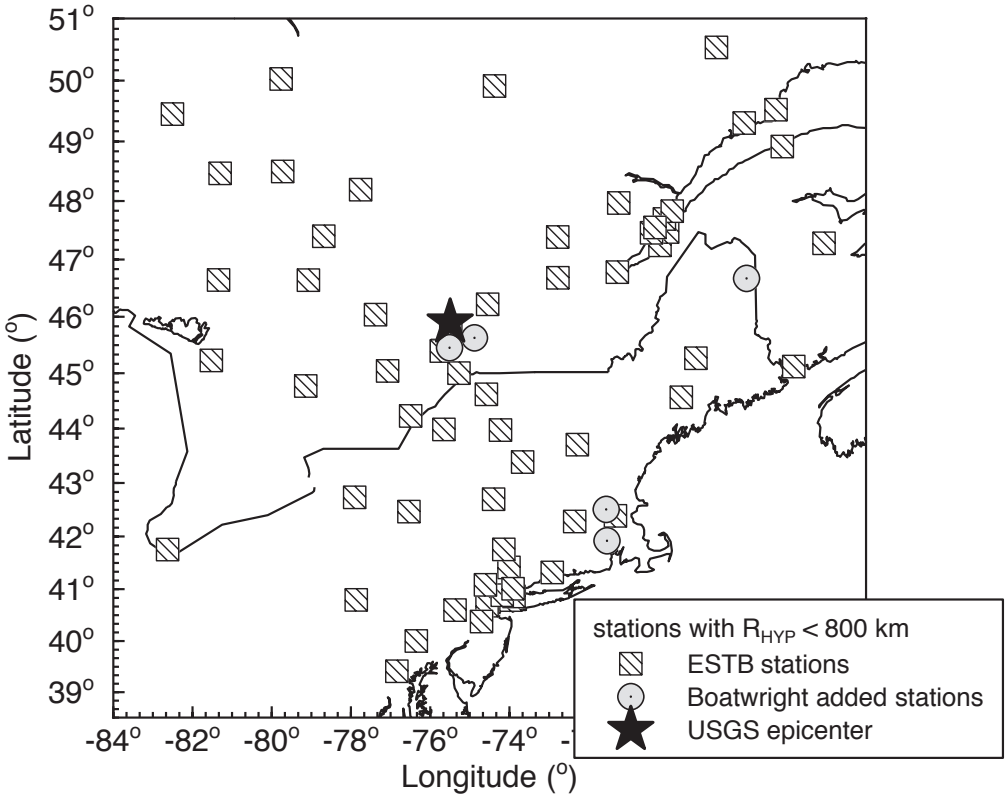

▲ **Figure 1.** Map of Val des Bois epicenter and stations for which data were used to determine $\Delta\sigma$.

The 23 August 2011 Mineral, Virginia, earthquake (**M** 5.8) occurred after this paper was in review. Although well recorded, data from that earthquake are not included in this paper because most of the recording sites are probably not hard rock sites, and therefore unknown site response may be more important in the analysis than for the data from the hard rock stations used here.

Most of the PSA values were the same as those used in Bea10. For the Saguenay earthquake, PSA values from recordings at stations S05 and S14 were not included, the first because it only recorded one horizontal component of motion, and the second because the record was triggered by the *S* wave. For the Saguenay earthquake, BS11 included some recordings from National Center for Earthquake Engineering Research (NCEER) stations in the northeastern United States, and I used PSA values computed from these recordings. For the Riviere du Loup and the Val des Bois earthquakes I used PSA values from the ESTB. For both of these events, I also used additional data from BS11 and Boatwright (personal communication 2011). In the Results section I give $\Delta\sigma$ for datasets without and with the additional BS11 and Boatwright data.

Maps of epicenters and stations that provided data for the analysis are given in Bea10 for all but the Val des Bois earthquake. A map of the earthquake locations and stations for that earthquake is given in Figure 1.

Plots of PSA vs. distance are given in Figures 2, 3, and 4 for the three earthquakes of prime concern here. The distance measure is intended to be the closest distance to the rupture surface (R_{RUP}), but the earthquakes are small enough and the distances to the stations are great enough that hypocentral distance has been used as a surrogate for R_{RUP}. The figures only show the 0.2 s and 2.0 s PSA, as the 0.1 s and 1.0 s plots are similar to the 0.2 s and 2.0 s plots, respectively. The symbols in the graphs indicate whether the data are from horizontal or vertical recordings (where a factor has been applied to the vertical components to approximate a horizontal component, as discussed in Bea10). The symbols also show additional data from BS11 and Boatwright, as well as stations they have classified as site class B. Figures 2, 3, and 4 clearly show the relative lack of data within 50 km, with the bulk of the data occurring at distances greater than about 200 km. The Riviere du Loup event has more recordings at distances less than 50 km than the other two events. The graphs also show that there is not an obvious difference in the vertical motions converted to horizontal motions (using the conversions of Siddiqqi and Atkinson 2002) and the horizontal motions, although simulations suggest that differences should occur (*e.g.*, Chapman and Godbee 2011). It is also noted that the additional data provided by BS11 and Boatwright are compatible with those used by Bea10 and those from the ESTB. Because of the similarity of the converted-to-horizontal vertical motions and the horizontal motions, both are used together in the inversion for $\Delta\sigma$.

METHODOLOGY

As explained in detail in Bea10, the stress parameter is determined by fitting the logarithm of the observed PSA for periods of 0.1 s and 0.2 s to simulated PSA, with the inversions done

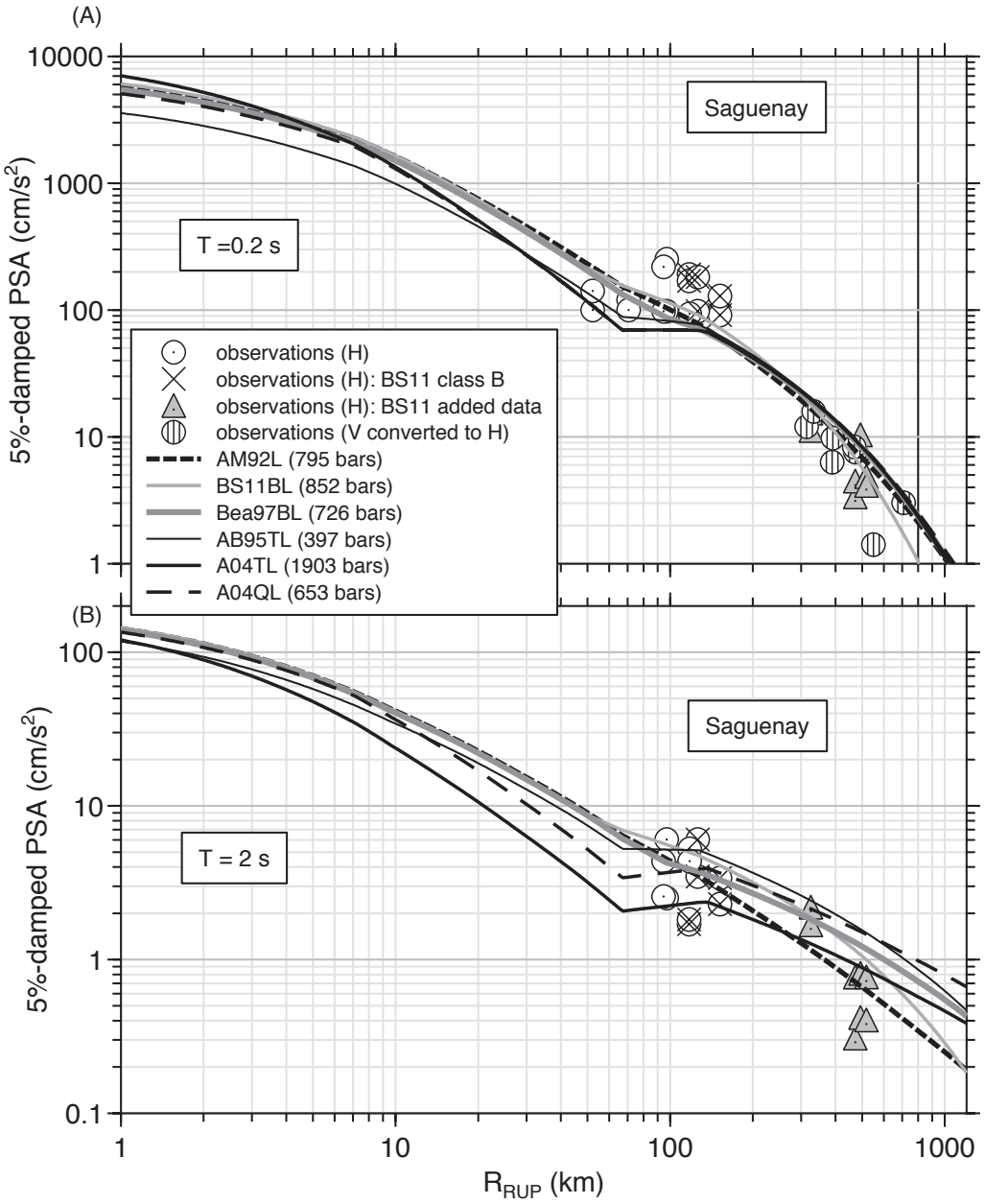

▲ **Figure 2.** Observations from the 1988 Saguenay earthquake (symbols) and simulated pseudo-absolute response spectral acceleration (PSA) for geometric mean of the stress parameter derived from inverting separately the 0.1 s and 0.2 s PSA observations. The abbreviations for the curves are defined in the footnote to Table 2. The vertical black line at 800 km in (A) indicates the upper limit of distance for data used in the inversion for $\Delta\sigma$ (it is not shown in (B) for T = 2.0 s because those data were not used in the inversion).

separately for each period. The inversions were done as follows: for a given earthquake and oscillator period, motions were simulated at the distance of each recording for a suite of stress parameters ($\Delta\sigma$), ranging from 6.25 bars to 3,200 bars; the residual $\log(PSA_{OBS}/PSA_{SIM})$ was computed for each observation for a given stress parameter, and the arithmetic average of all residuals for rock stations within 800 km that recorded the earthquake was computed, treating each observation as an independent variable; a second-order polynomial with $\log\Delta\sigma$ as the variable was fit to the average residuals, and this quadratic was solved for the value of $\log\Delta\sigma$ that gave zero residual.

With a few exceptions, I used the same model parameters and random-vibration stochastic-method simulation program (SMSIM, Boore 2005) as used in Bea10; the model parameters are given in Tables 2, 3, and 4 of Bea10. A single-corner-frequency source model was used. Because of restricting the analysis to hard rock sites, the results should not be sensitive to site amplification and κ_0 (for which I used a value of 0.005 s). The simulation programs include new determinations of the durations used to compute root-mean-square oscillator response in the random-vibration calculations (Boore and Thompson forthcoming), but for the magnitudes, distances, and periods

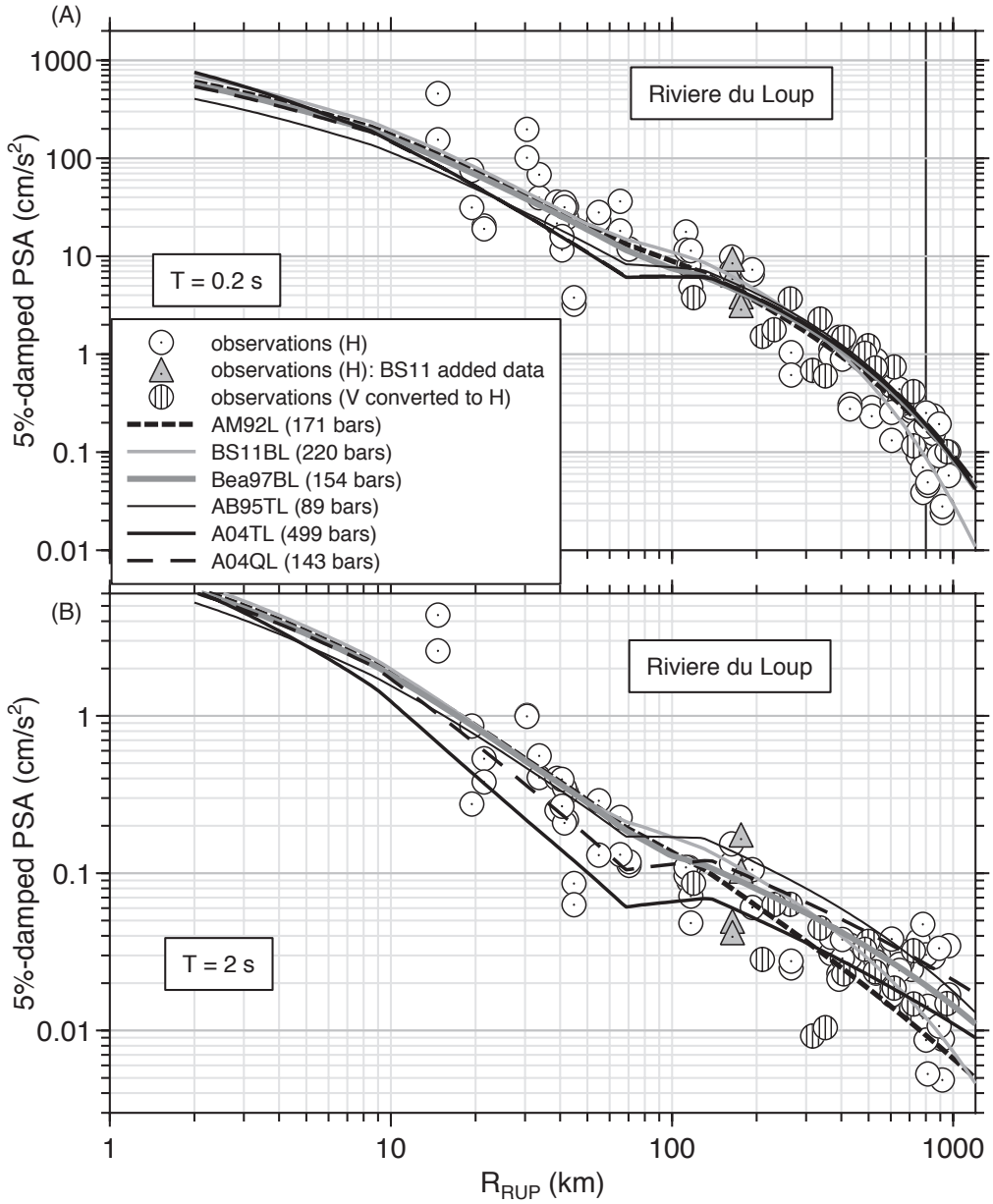

▲ **Figure 3.** Observations from the 2005 Riviere du Loup earthquake (symbols) and simulated pseudo-absolute response spectral acceleration (PSA) for geometric mean of the stress parameter derived from inverting separately the 0.1 s and 0.2 s PSA observations. The abbreviations for the curves are defined in the footnote to Table 2. The vertical black line at 800 km in (A) indicates the upper limit of distance for data used in the inversion for $\Delta\sigma$ (it is not shown in (B) for T = 2.0 s because those data were not used in the inversion).

used here the PSA simulations are similar to those from the previous method of computing durations.

The most important change from the Bea10 models is the consideration of more attenuation models. These models are made up of geometrical spreading and Q operators and can be divided into groups according to the number of line segments used to describe the geometrical spreading when the logarithm of the Fourier amplitude spectrum is plotted against the logarithm of distance (Atkinson 2012, this issue). The attenuation models used in this paper are given in Table 2. I used the models as published, without adjusting the coefficients to better fit the data. There are two linear models. The Q value in the AM92L model was determined by fitting the attenuation of many small earthquakes, whereas that in Bea10L came from approximating the A04TL attenuation (which in turn was based on data from numerous small events). Bilinear models (first used by Street *et al.* 1975) have two segments of geometrical spreading separated by a hinge distance. The four bilinear models considered here have hinge distances of 50, 60, and 100 km. The coefficients in the BS11 bilinear model were determined from data for some of the earthquakes considered in this paper, whereas those for the other models were determined from smaller earthquakes. I used three trilinear models. The AB95TL model has an initial spreading going as $1/R$, whereas that in AB95TL13 and

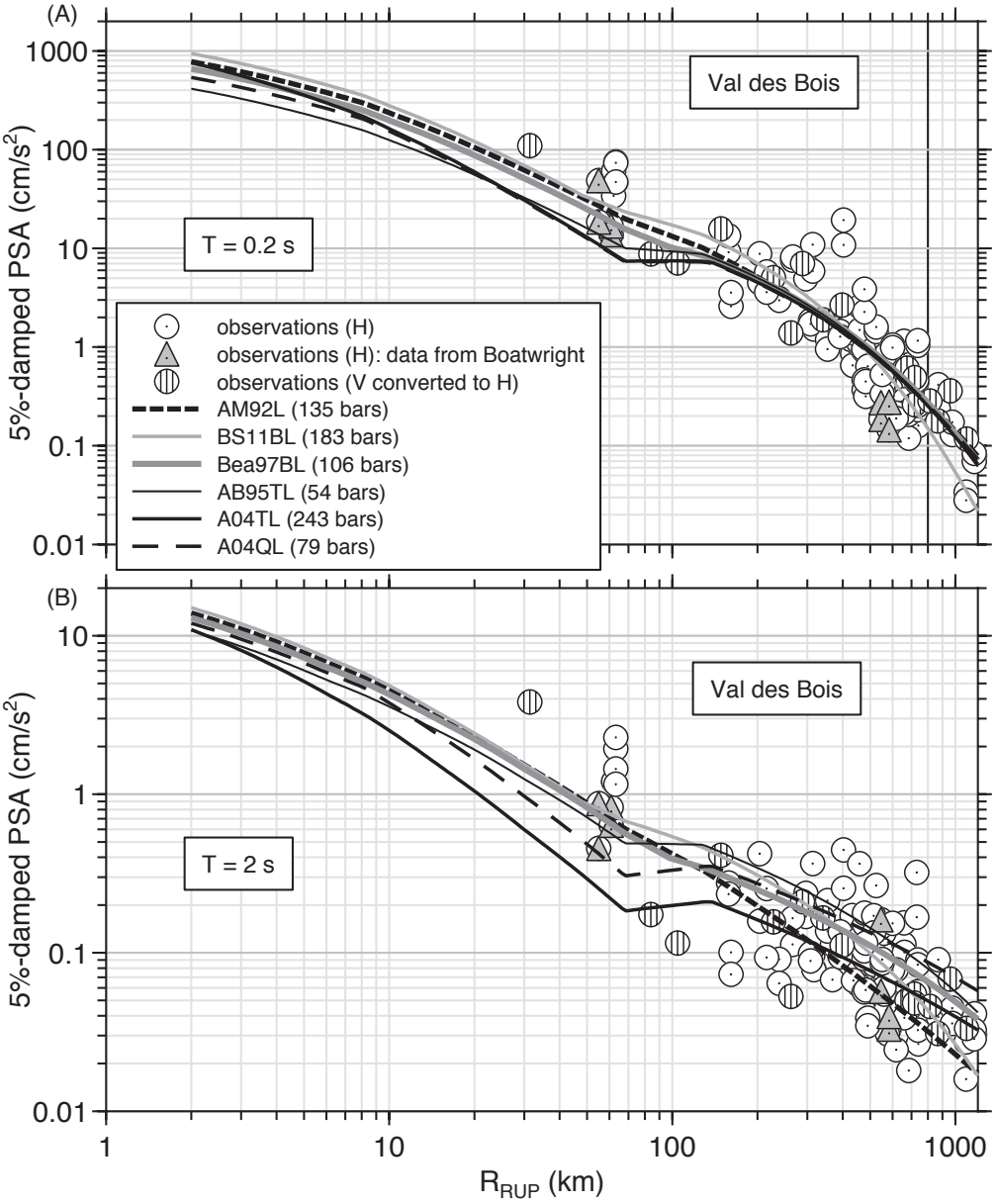

▲ **Figure 4.** Observations from the 2010 Val des Bois earthquake (symbols) and simulated pseudo-absolute response spectral acceleration (PSA) for geometric mean of the stress parameter derived from inverting separately the 0.1 s and 0.2 s PSA observations. The abbreviations for the curves are defined in the footnote to Table 2. The vertical black line at 800 km in (A) indicates the upper limit of distance for data used in the inversion for $\Delta\sigma$ (it is not shown in (B) for T = 2.0 s because those data were not used in the inversion).

A04TL go as $1/R^{1.3}$ (the spreading coefficient for the first segment in A04TL comes from the analysis of data, whereas that in AB95TL13 comes from a modification of AB95TL suggested by Atkinson 2012). The final model (A04QL) is a modification of A04TL suggested by Atkinson and Assatourians (2010), in which the geometrical spreading goes as $1/R$ within 10 km. The Q function for A04TL and A04QL is a fit to the Q values in Table 2 of Atkinson (2004) and was devised for use in the SMSIM stochastic-method simulation program.

For each earthquake, stress parameters ($\Delta\sigma$) were determined for the ten attenuation models in Table 2. After $\Delta\sigma$ was determined for each dataset and attenuation function, the geometric mean of the $\Delta\sigma$ independently determined for the 0.1 s and 0.2 s PSA was used to simulate PSA vs. distance for oscillator periods of 0.1 s, 0.2 s, 1.0 s, and 2.0 s. In the simulations, the Toro (2002) modification to distance was used to convert the hypocentral distance to an effective distance that is intended to include finite-fault effects in the point-source stochastic-method simulations (the one exception to this is for the Nahanni earthquake, for which the distances assigned to three near-fault observations have been modified to account for finite-fault effects—see Bea10; a further modification to these distances in the simulations would be incorrect). The distance used in the plots of point-source simulations for a finite fault is often R_{RUP}, consistent with the functional forms used in many ground-motion prediction equations, but in the simulations of

ground motion for a given R_{RUP}, that distance should be modified to account for finite-fault effects; this modification can use R_{EFF} of Boore (2009) when the fault-station geometry is known, or generic modifications such as those of Atkinson and Silva (2000) or Toro (2002). Having said that, the modification to the distance has a negligible effect on the derived $\Delta\sigma$ because the observations are at distances such that the modified and the original distances are essentially the same. The modified distances do affect the shape of the simulated curves at close distances, however, when R_{RUP} is used for the abscissa, as it is in Figures 2, 3, and 4: the curves tend to flatten as distance decreases, whereas without the modification the curves would continue to rise with decreasing distance.

RESULTS

The geometric-mean $\Delta\sigma$ of the stress parameters, determined independently from the 0.1 s and 0.2 s PSA observations, are given in Tables 3 through 5 for the Saguenay, Riviere du Loup, and Val des Bois earthquakes. Results are given for each of the ten attenuation models. In order to assess the sensitivity of the derived results to the datasets, Tables 3 through 5 contain separate values of the stress for various datasets. Also included are the standard deviations of the residuals about the predicted values of PSA using the inverted stress for each model. Table 6 contains stresses and standard deviations for the nine earthquakes studied in this paper. The stresses for the Saguenay, Riviere du Loup, and Val des Bois earthquakes are carried over from the second row in Tables 3, 4, and 5, respectively.

For the Saguenay earthquake, Table 3 gives a value of stress for the model parameters used by BS11. These model parameters differ from those used by Bea10 in five ways: (1) the source velocity was 3.8 rather than 3. 7 km/s; (2) the radiation pattern was 0.58 rather than 0.55; (3) the hard rock crustal and site amplification was somewhat different; (4) the conversion between moment and moment magnitude was slightly different, such that I had to use **M** 5.83 in my software in order for the seismic moments to be the same; and (5) BS11 only used data within 626 km, whereas the other determinations of $\Delta\sigma$ used data within 800 km. The value of 597 bars is higher than the 419±68 bars in BS11. The difference might be due to my exclusion of the BS11 class B data, or it may be due to deriving $\Delta\sigma$ from the average distance-corrected Fourier acceleration spectra, as in BS11, rather than individual PSA at each recording site. Further investigation of the reason for the difference in $\Delta\sigma$ is beyond the scope of this paper.

The simulated and observed motions for $\Delta\sigma$ from a subset of six attenuation models and one dataset (the Bea10 dataset with the additions of BS11 or Boatwright data) are compared in Figures 2 through 4. The figures contain two graphs for the three earthquakes: the first graph is for one of the oscillator periods used to derive $\Delta\sigma$ (0.2 s) and the second graph shows observations and simulations for a period of 2.0 s. The longer-period data were not used in deriving $\Delta\sigma$, and the graphs of the 2.0 s PSA are included as a result of suggestions by Atkinson and Assatourians (2010), Assatourians and Atkinson (2010), and Atkinson (2012) that the comparison of observations and simulations at longer periods could help discriminate between the various attenuation models, since seismic moment is an independent constraint (the same reasoning was used by Boore *et al.* 2009). The distance axes in the figures were chosen so as to display the simulations at close distances at the expense of detail in the fit of data and simulations. Note that the curves of simulated motion use the geometric mean of the stress param-

TABLE 2
Attenuation Model Parameters*

Model	Type	b	Hinge Distances (km)	Q	β (km/s)
AM92L	Linear	–1.0	n/a	2000	3.8
Bea10L	Linear	–1.0	n/a	2850	3.7
BS11BL	Bilinear	–1.0, –0.5	50	$410f^{0.5}$	3.5
AM92BL	Bilinear	–1.0, –0.5	60	$790f^{0.27}$	3.8
BA92BL	Bilinear	–1.0, –0.5	100	$755f^{0.52}$	3.5
Bea97BL	Bilinear	–1.0, –0.5	100	$962f^{0.22}$	3.5
AB95TL	Trilinear	–1.0, 0.0, –0.5	70, 130	$680f^{0.36}$	3.8
AB95TL13	Trilinear	–1.3, 0.0, –0.5	70, 130	Same as AB95	3.8
A04TL	Trilinear	–1.3, 0.2, –0.5	70, 140	$844f^{-1.2}$: $f \le 0.86$ Hz $1034f^{0.14}$: 0.86 Hz < f $536f^{0.55}$: 5 Hz < f	3.7
A04QL	Quadlinear	–1.0, –1.3, 0.2, –0.5	10, 70, 140	Same as A04TL	3.7

* The geometric spreading function is piecewise continuous, with the distance dependence in each segment given by R^b. The anelastic function is $\exp(-\pi R/Q\beta)$. A04 = Atkinson (2004); AB95 = Atkinson and Boore (1995); AM92 = Atkinson and Mereu (1992); BA92 = Boore and Atkinson (1992); Bea97 = Benz *et al.* (1997); Bea10 = Boore *et al.* (2010); BS11 = Boatwright and Seekins (2011).

eters derived for periods of 0.1 s and 0.2 s and therefore will not fit the 0.2 s PSA observations as well as the $\Delta\sigma$ derived for that period. As shown in Bea10, however, the difference in $\Delta\sigma$ for the two periods is relatively small, and thus there will not be a large difference between the curves shown in the figures and those for the optimum stress parameter for each period. Also note in the figures that the curves for the $1/R$ attenuation model (AM92L) show some apparent non-$1/R$ attenuation, consisting of changes in slope at 10, 70, and 130 km; this is due to the path duration, as discussed in Bea10, which has slope changes at these three distances.

DISCUSSIONS AND CONCLUSIONS

The results given in Tables 3 through 6 confirm what was found in Bea10: the stress parameter depends on the attenuation model (as well as the other model parameters). As an example, note that the stress parameters for the A04TL and A04QL differ by a factor of about 3, although the two models differ from one another only within 10 km. Given that there are no data within 10 km, this result may seem paradoxical, but it is easily explained. The two attenuation models only differ inside of 10 km (with geometrical spreading of $1/R^{1.3}$ and $1/R$

TABLE 3
Stress parameter ($\Delta\sigma$) and standard deviation of residuals (σ_{RSDL}) for the 1988 Saguenay earthquake*

Dataset/Atten. Model	AM92L	Bea10L	BS11BL	AM92BL	BA92BL	Bea97BL	AB95TL	AB95TL13	A04TL	A04QL
$\Delta\sigma$ (bars)										
Bea10′	861	667	879	622	581	843	481	3404	2444	839
Bea10′, add NCEER	795	577	852	531	458	726	397	2829	1903	653
Bea10′, xBS11 class B	668	503	727	481	423	637	383	2703	1926	662
Bea10′, xBS11 class B, add NCEER	654	459	741	428	348	576	324	2308	1522	522
as above, BS11 params	—	—	597	—	—	—	—	—	—	—
σ_{RSDL}										
Bea10′	0.24	0.25	0.22	0.25	0.30	0.26	0.26	0.26	0.29	0.29
Bea10′, add NCEER	0.24	0.25	0.23	0.26	0.31	0.26	0.27	0.27	0.30	0.30
Bea10′, xBS11 class B	0.21	0.23	0.21	0.23	0.28	0.24	0.26	0.25	0.29	0.30
Bea10′, xBS11 class B, add NCEER	0.21	0.23	0.22	0.23	0.27	0.24	0.26	0.25	0.29	0.29
as above, BS11 params	—	—	0.20	—	—	—	—	—	—	—

* Bea10′ = the dataset used by Boore *et al.* (2010), minus stations S05 and S14; add NCEER = add site class A NCEER data from Boatwright and Seekins (2011); xBS11= remove Bea10′ data classified as site class other than A by BS11; BS11 params = the inversion for $\Delta\sigma$ used BS11 parameters for source velocity, radiation pattern, and site class A amplifications. σ_{RSDL} = the standard deviation of the residuals between observed and simulated log*PSA* (base 10 logarithms).

TABLE 4
Stress parameter ($\Delta\sigma$) and standard deviation of residuals (σ_{RSDL}) for the 2005 Riviere du Loup earthquake*

Dataset/Atten. Model	AM92L	Bea10L	BS11BL	AM92BL	BA92BL	Bea97BL	AB95TL	AB95TL13	A04TL	A04QL
$\Delta\sigma$ (bars)										
ESTB	170	116	226	119	88	153	90	801	503	144
ESTB, add BS11 data	171	117	220	119	90	154	89	796	499	143
ESTB, BS11 class A	175	117	237	121	88	157	91	818	505	144
ESTB, BS11 class A, add BS11 data	171	120	222	124	95	158	96	842	546	156
σ_{RSDL}										
ESTB	0.29	0.31	0.29	0.30	0.34	0.30	0.32	0.30	0.34	0.35
ESTB, add BS11 data	0.28	0.30	0.29	0.30	0.34	0.29	0.31	0.30	0.34	0.34
ESTB, BS11 class A	0.28	0.30	0.29	0.29	0.34	0.29	0.31	0.30	0.33	0.34
ESTB, BS11 class A, add BS11 data	0.29	0.31	0.28	0.30	0.35	0.30	0.32	0.31	0.35	0.35

* ESTB = Engineering Seismology Toolbox (see Data and Resources section); BS11 = Boatwright and Seekins (2011).

TABLE 5
Stress parameter ($\Delta\sigma$) and standard deviation of residuals (σ_{RSDL}) for the 2010 Val des Bois earthquake*

Dataset/Attenuation Model	AM92L	Bea10L	BS11BL	AM92BL	BA92BL	Bea97BL	AB95TL	AB95TL13	A04TL	A04QL
$\Delta\sigma$ (bars)										
ESTB	145	87	197	82	56	114	57	455	251	82
ESTB, add Boat data	135	82	183	78	53	106	54	432	243	79
ESTB, Boat class A	140	84	189	79	54	109	54	434	239	78
ESTB, Boat class A, add Boat data	128	78	174	74	51	101	52	411	231	75
σ_{RSDL}										
ESTB	0.30	0.32	0.29	0.31	0.34	0.31	0.33	0.32	0.35	0.35
ESTB, add Boat data	0.30	0.32	0.30	0.32	0.35	0.31	0.33	0.33	0.35	0.36
ESTB, Boat class A	0.30	0.31	0.30	0.31	0.34	0.31	0.32	0.32	0.34	0.34
ESTB, Boat class A, add Boat data	0.30	0.32	0.30	0.32	0.35	0.31	0.33	0.33	0.35	0.35

* ESTB = Engineering Seismology Toolbox (see Data and Resources section); Boat = data provided by J. Boatwright (personal communication 2011).

TABLE 6
Stress parameter ($\Delta\sigma$) and standard deviation of residuals (σ_{RSDL}) for the nine events, along with the geometric means of $\Delta\sigma$ computed with and without the Saguenay $\Delta\sigma$.

Dataset/Attenuation Model	AM92L	Bea10L	BS11BL	AM92BL	BA92BL	Bea97BL	AB95TL	AB95TL13	A04TL	A04QL
$\Delta\sigma$										
Nahanni	53	52	56	54	53	54	54	146	145	60
Saguenay	795	577	852	531	458	726	397	2829	1903	653
Mt. Laurier	155	104	166	91	72	130	63	562	330	99
Cap Rouge	71	43	93	40	29	59	27	263	137	40
St. Anne des Monts	60	36	79	34	24	49	24	215	116	35
Kipawa	82	47	127	46	29	64	31	265	136	43
Ausable Forks	100	69	99	58	48	82	40	302	183	61
Riviere du Loup	171	117	220	119	90	154	89	796	499	143
Val des Bois	135	82	183	78	53	106	54	432	243	79
geom. mean $\Delta\sigma$ (w/ Sag.)	122	82	148	77	59	104	56	422	258	83
geom. mean $\Delta\sigma$ (w/o Sag.)	96	64	118	61	46	82	44	333	201	64
σ_{RSDL}										
Nahanni	0.49	0.49	0.50	0.49	0.49	0.49	0.49	0.50	0.50	0.50
Saguenay	0.24	0.25	0.23	0.26	0.31	0.26	0.27	0.27	0.30	0.30
Mt. Laurier	0.21	0.20	0.21	0.19	0.22	0.20	0.20	0.20	0.21	0.21
Cap Rouge	0.25	0.28	0.25	0.26	0.31	0.26	0.27	0.26	0.29	0.29
St. Anne des Monts	0.28	0.30	0.27	0.29	0.33	0.29	0.29	0.29	0.32	0.32
Kipawa	0.19	0.20	0.24	0.20	0.22	0.20	0.20	0.20	0.21	0.21
Ausable Forks	0.22	0.23	0.23	0.23	0.25	0.23	0.24	0.24	0.25	0.25
Riviere du Loup	0.28	0.30	0.29	0.30	0.34	0.29	0.31	0.30	0.34	0.34
Val des Bois	0.30	0.32	0.30	0.32	0.35	0.31	0.33	0.33	0.35	0.36

for A04TL and A04QL, respectively), and because they fit data that is only at distances greater than 10 km, the curves will be the same for distances of 10 km or greater. The values of $\Delta\sigma$ are determined by the curves extrapolated back to a distance of 1 km, however, where the ratio of the amplitudes will be $10^{0.3} = 2$ (the divergence of the A04TL and A04QL models as distance decreases can be seen in parts A of Figures 2 through 4). The stress parameter is proportional to high-frequency spectral level to the 1.5 power, so the ratio of the stresses for the two attenuation laws will be $2^{1.5} = 2.8$. Similar considerations apply to differences in $\Delta\sigma$ for the other attenuation models.

Several other general conclusions can be drawn from Table 6 and Figures 2 through 4. As expected from the standard deviations in the table, the fits to the 0.2 s PSA data shown in the figures are generally comparable for the various attenuation models, although the stress parameters can differ substantially. The best fits in general are for the linear and bilinear models, with the AM92L and BS11BL models having somewhat smaller standard deviations than the other models. Focusing on the three earthquakes being given special attention, the A04TL and A04QL models give somewhat poorer overall fits to the 0.1 s and 0.2 s PSA observations than the other attenuation models.

It is also important to note from Figures 2 through 4 that the biggest differences in the predicted short-period motions are at distances between about 10 and 100 km, with the motions from models having $1/R^{1.3}$ spreading significantly less than for the other models. This is an important distance range for engineering applications, and clearly more data are needed to determine the proper model of geometrical spreading.

Tables 3 through 5 provide some insight into the sensitivity of $\Delta\sigma$ to the datasets used in the inversion, as well as the attenuation models (and other model parameters, as discussed earlier when comparing results for Saguenay when using the Bea10 and the BS11 parameters). As shown in Table 3, including the NCEER data for the Saguenay earthquake leads to a factor of about 3% to 22% reduction in stress, depending on the attenuation model; excluding the sites classified as B by BS11 leads to a comparable reduction. The combined effect of including NCEER data and excluding class B gives a reduction of 16% to 38%, depending on the attenuation model. The dependence of $\Delta\sigma$ on the dataset is not as pronounced for the Riviere du Loup and Val des Bois events, probably because there is a better distribution of data with distance and azimuth and because relatively fewer data were added or removed from the Bea10' and ESTB datasets.

The longer-period motions (1.0 s and 2.0 s) are not as sensitive to the stress parameter and the Q function as the short-period motions (0.1 s and 0.2 s). As Figures 2, 3, and 4 show, the predictions for the various models approach one another at short distances, as they should given that the seismic moment is the same for each model. The Riviere du Loup earthquake has the most recordings at distances within 100 km, and a subjective, visual examination of Figure 3B suggests that the A04QL model best agrees with the observations for this earthquake. This would give support to the more rapid geometrical spreading for this model than in models having $1/R$ spreading out to distances of 50 km or more. Note also that the A04QL model gives a significantly better fit to the data than does the A04TL model; both models have similar amplitudes at close distances (being constrained by the moment), but the A04TL motions decay more rapidly with increasing distance than the A04QL motions within the first 10 km, leading to A04TL motions that are less than those from A04QL at the distances for which the data are available. The A04TL and A04QL models, however, fit the shorter-period motions less well than do the other attenuation models. One way of resolving this difference in short-period and long-period fits is to use frequency-dependent geometrical spreading in the simulations. Currently available stochastic-method simulation programs do not allow for this, however, but the SMSIM programs are being modified to include frequency-dependent geometrical spreading. Overall, the conclusions in this paper are similar to those in Atkinson (2012): no one attenuation model provides the best fit to all earthquakes and to all periods of motion. There are insufficient observations at distances within 100 km to better constrain the attenuation model, and therefore simple linear geometrical spreading models going as $1/R$ are a reasonable alternative to more complex models for predictions over a suite of earthquakes and regions. The conclusion that the $1/R$ attenuation model can be used in lieu of the more complex models is certain to change as more data are collected, with the strong possibility that the best attenuation models will be regionally dependent. A final conclusion is that simulations of motions from future earthquakes using stress parameters (or distributions of stress parameters) derived from existing data must include all the model parameters used in deriving those stress parameters. This includes the source velocity and density, the average radiation pattern, crustal and site amplifications, and path-dependent duration.

A final point is worth mentioning: all of the simulations in this paper used a point-source model that does not specifically include rupture- and wave-propagation effects, such as directivity and the interaction of various seismic phases. For example, directivity has been proposed to explain the high values of short-period motions in the 100 km to 150 km range for the Saguenay earthquake (*e.g.*, Haddon 1992; see the high values can be seen in Figure 2A of this paper), but in the model used here, such effects will be mapped into the derived $\Delta\sigma$ and the aleatory variability. The uses of the simulation model must be kept in mind; the point-source stochastic model with stresses and aleatory variability as determined in this paper might be appropriate for applications in which generic, region-specific ground-motion prediction equations are developed for use in constructing seismic hazard maps (this is a common and widely used application), but the model might be inappropriate for simulations of motions for a particular earthquake-station combination in which the kinematic or dynamic properties of the rupture over a finite-fault surface are specified.

DATA AND RESOURCES

The response spectral values came from the electronic supplement of AB06 (http://bssa.geoscienceworld.org/cgi/content/

full/96/6/2181/DC1), the Engineering Seismology Toolbox (http://www.seismotoolbox.ca), and my calculations from time series provided by Jack Boatwright and Linda Seekins of the U.S. Geological Survey.

The depth and moment magnitude (**M** 5.07) of the Val des Bois earthquake come from R. Herrmann (http://www.eas.slu.edu/eqc/eqc_mt/MECH.NA/20100623174142/index.html, last accessed November 2011), where his moment (M_0) of 4.57e23 dyne-cm has been converted to moment magnitude using the relation $\mathbf{M} = (2/3)(\log M_0 - 16.05)$ (Hanks and Kanamori 1979).

The SMSIM programs used for the simulations can be obtained from the online software link on http://www.daveboore.com (last accessed November 2011).

ACKNOWLEDGMENTS

I thank Jack Boatwright and Linda Seekins for providing data and for useful discussions. I also thank Gail Atkinson for sharing a preprint of her paper in advance of publication, as well as stimulating discussions and comments on the manuscript. I also thank Ken Campbell, John Douglas, and Art Frankel for their comments, and Karen Assatourians for reviewing the paper, as well as processing and archiving the data available from the Engineering Seismology Toolbox Web site.

REFERENCES

Assatourians, K., and G. Atkinson (2010). Database of processed time series and response spectra for Canada: An example application to study of the 2005 *MN* 5.4 Riviere du Loup, Quebec earthquake. *Seismological Research Letters* **81**, 1,013–1,031.

Atkinson, G. M. (2004). Empirical attenuation of ground-motion spectral amplitudes in southeastern Canada and the northeastern United States. *Bulletin of the Seismological Society of America* **94,** 1,079–1,095.

Atkinson, G. M. (2012). Evaluation of attenuation models for the northeastern United States/southeastern Canada. *Seismological Research Letters* **83** (1), 166–178.

Atkinson, G. M., and K. Assatourians (2010). Attenuation and source characteristics of the 23 June 2010 **M** 5.0 Val-des-Bois, Quebec, earthquake. *Seismological Research Letters* **81**, 849–860.

Atkinson, G. M., and D. M. Boore (1995). Ground motion relations for eastern North America. *Bulletin of the Seismological Society of America* **85**, 17–30.

Atkinson, G., and R. Mereu (1992). The shape of ground motion attenuation curves in southeastern Canada. *Bulletin of the Seismological Society of America* **82**, 2,014–2,031.

Atkinson, G. M., and W. Silva (2000). Stochastic modeling of California ground motions. *Bulletin of the Seismological Society of America* **90**, 255–274.

Benz, H. M., A. Frankel, and D. M. Boore (1997). Regional *Lg* attenuation for the continental United States. *Bulletin of the Seismological Society of America* **87**, 606–619.

Boatwright, J., and L. Seekins (2011). Regional spectral analysis of three moderate earthquakes in northeastern North America. *Bulletin of the Seismological Society of America* **101**, 1,769–1,782.

Boore, D. M. (2003). Prediction of ground motion using the stochastic method. *Pure and Applied Geophysics* **160**, 635–676.

Boore, D. M. (2005). *SMSIM—Fortran Programs for Simulating Ground Motions from Earthquakes: Version 2.3—A Revision of OFR 96-80-A, U.S. Geological Survey Open-File Report*. USGS Open-File Report 00-509, revised 15 August 2005, 55 pp.

Boore, D. M. (2009). Comparing stochastic point-source and finite-source ground-motion simulations: SMSIM and EXSIM. *Bulletin of the Seismological Society of America* **99**, 3,202–3,216.

Boore, D. M., and G. M. Atkinson (1992). Source spectra for the 1988 Saguenay, Quebec, earthquakes. *Bulletin of the Seismological Society of America* **82**, 683–719.

Boore, D. M., K. W. Campbell, and G. M. Atkinson (2010). Determination of stress parameters for eight well-recorded earthquakes in eastern North America. *Bulletin of the Seismological Society of America* **100**, 1,632–1,645.

Boore, D. M., A. Skarlatoudis, B. Margaris, C. Papazachos, and C. Ventouzi (2009). Along-arc and back-arc attenuation, site response, and source spectrum for the intermediate-depth January 8, 2006, **M** 6.7 Kythera, Greece, earthquake. *Bulletin of the Seismological Society of America* **99**, 2,410–2,434.

Boore, D. M., and E. M. Thompson (forthcoming). Empirical improvements for estimating earthquake response spectra with random vibration theory. *Bulletin of the Seismological Society of America* **102**.

Chapman, M. C., and R. W. Godbee (2011). Modeling near-source geometrical spreading and the relative amplitudes of vertical and horizontal high-frequency ground motions in eastern North America.

Haddon, R. A. W. (1992). Waveform modeling of strong-motion data for the Saguenay earthquake of 25 November 1988. *Bulletin of the Seismological Society of America* **82**, 720–754.

Hanks, T. C., and H. Kanamori (1979). A moment magnitude scale. *Journal of Geophysical Research* **84**, 2,348–2,350.

Siddiqqi, J., and G. Atkinson (2002). Ground motion amplification at rock sites across Canada, as determined from the horizontal-to-vertical component ratio. Bulletin of the Seismological Society of America 92, 877–884.

Street, R. L., R. B. Herrmann, and O. W. Nuttli (1975). Spectral characteristics of the *Lg* wave generated by central United States earthquakes. Geophysical Journal of the Royal Astronomical Society 41, 51–63.

Toro, G. R. (2002). Modification of the Toro et al. (1997) Attenuation Relations for Large Magnitudes and Short Distances. Risk Engineering, Inc. report; http://www.riskeng.com/PDF/atten_toro_extended.pdf.

U.S. Geological Survey
MS 977
345 Middlefield Road
Menlo Park, California 94025 U.S.A.
boore@usgs.gov